Higgs to di-photons at ATLAS

B. Mellado
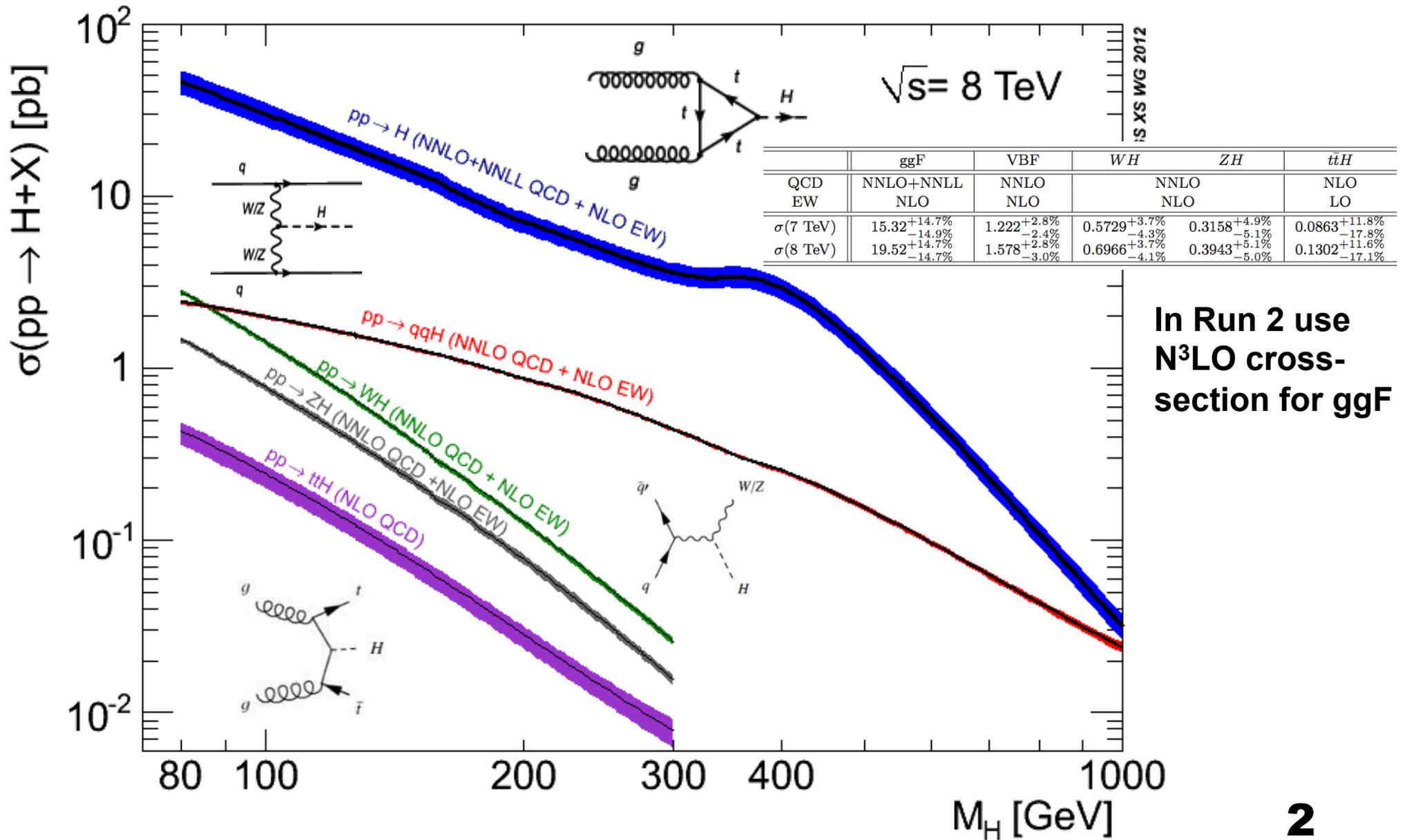## University of the Witwatersrand
On behalf of the ATLAS Collaboration
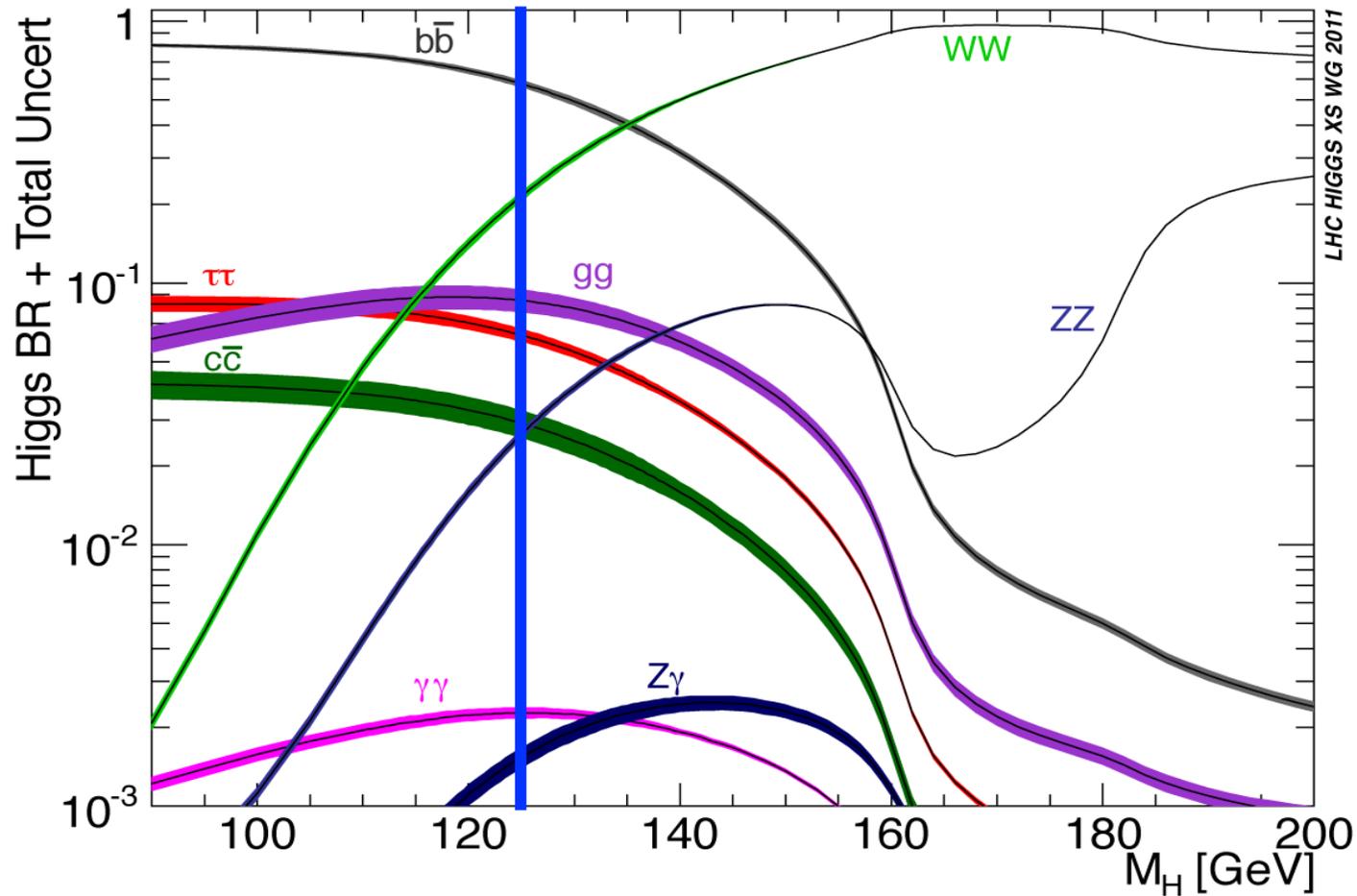
Higgs Couplings 2016, SLAC, 11/09/16
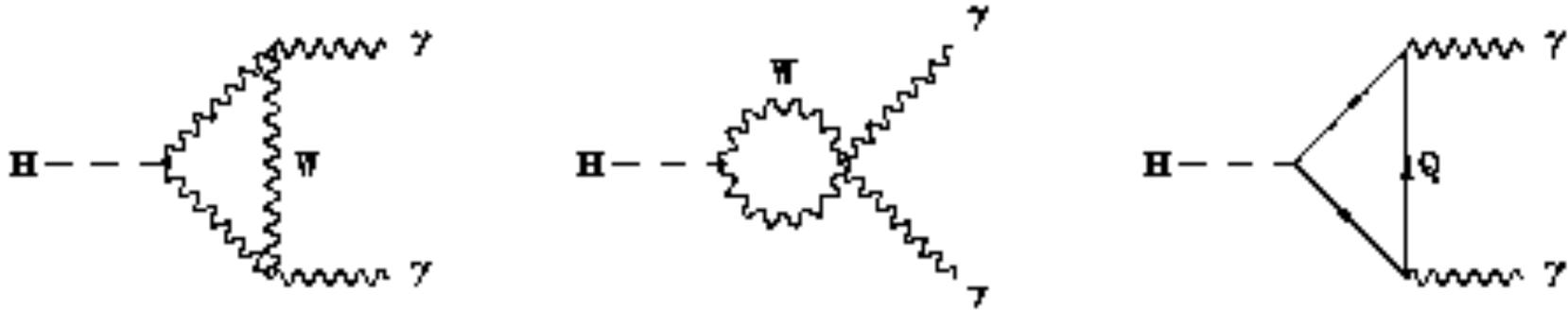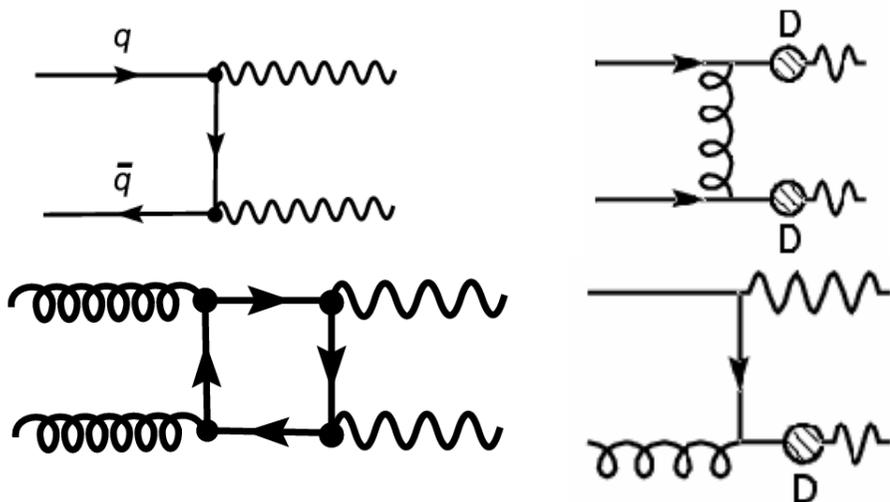
Higgs Cross-Sections at LHC

In Run 2 use N³LO cross-section for ggF

2

Main Decay Modes

B_b	B_τ	B_μ	B_c	B_g
$0.577^{+3.2\%}_{-3.3\%}$	$0.0632^{+5.7\%}_{-5.7\%}$	$(2.2\times10^{-4})^{+6.0\%}_{-5.9\%}$	$0.0291^{+12.2\%}_{-12.2\%}$	$0.0857^{+10.2\%}_{-10.0\%}$

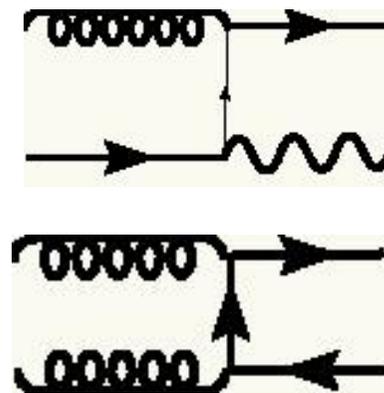| B_γ	$B_{Z\gamma}$	B_W	B_Z	$\Gamma_H\,[\,\mathrm{MeV}\,]$
$(2.28\times10^{-3})^{+5.0\%}_{-4.8\%}$	$(2.28\times10^{-3})^{+9.0\%}_{-8.8\%}$	$^{+4.3\%}_{-4.2\%}$	$2.64^{+4.3\%}_{-4.2\%}$	$4.07^{+4.0\%}_{-3.9\%}$

Higgs decay to γγ

γγ Backgrounds

Reducible γj and jj Backgrounds

$q \rightarrow \pi^0$

Different background components studied with data-driven methods

The ATLAS Detector
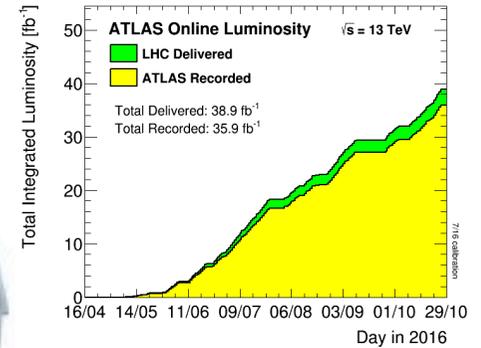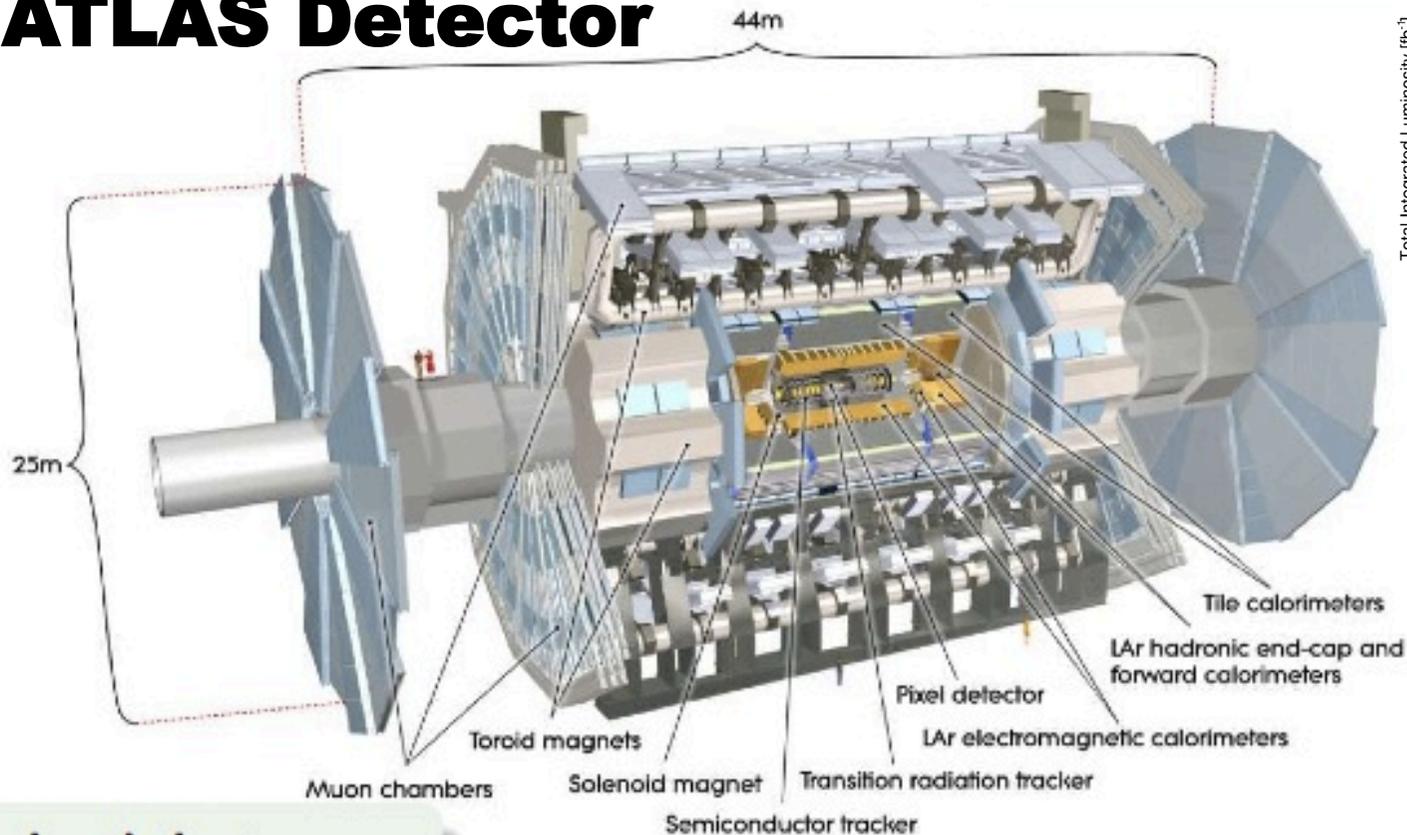
Inner detector :
Pixel detector + SCT + TRT
$$\frac{\sigma_{p_T}}{p_T} \approx 0.05\% p_T \oplus 1\% \,.\, |\eta| < 2.5$$

EM calorimeter :
Lead-LAr sampling calo. with accordion geometry
$$\frac{\sigma_E}{E} \approx \frac{10\%}{\sqrt{E}} \oplus 0.7\% \,.\, |\eta| < 3.2$$

Hadronic calorimeter :
Steel and scintillating tiles in the barrel, copper and liquid argon in end-caps
$$\frac{\sigma_E}{E} = \frac{50\%}{\sqrt{E}} \oplus 3\%, |\eta| < 3.2$$
$$\frac{\sigma_E}{E} = \frac{100\%}{\sqrt{E}} \oplus 10\%, 3.1 < |\eta| < 4.9$$

Muon spectrometer :
superconducting air-core toroid magnets, gaz based muon chambers
$$\frac{\sigma_{p_T}}{p_T} \approx 2\% \text{ at } 50\text{GeV to } 10\% \text{ at } 1\text{TeV}, |\eta| < 2.7$$

44m

25m

Tile calorimeters

LAr hadronic end-cap and forward calorimeters

Pixel detector

LAr electromagnetic calorimeters

Transition radiation tracker

Toroid magnets

Solenoid magnet

Semiconductor tracker

Muon chambers

ATLAS Online Luminosity $\sqrt{s}$ = 13 TeV
LHC Delivered
ATLAS Recorded
Total Delivered: 38.9 fb⁻¹
Total Recorded: 35.9 fb⁻¹

Total Integrated Luminosity [fb⁻¹]

16/04 14/05 11/06 09/07 06/08 03/09 01/10 29/10
Day in 2016

5

Object and Event Selection

□**Photons: EM clusters with calo + track isolation that:**

$$|\eta_\gamma| < 1.37 \text{ or } 1.52 < |\eta_\gamma| < 2.37$$

$$p_T^{\gamma_1}/m_{\gamma\gamma} > 0.35 \text{ and } p_T^{\gamma_2}/m_{\gamma\gamma} > 0.25$$

□**Leptons: Calo. + track isolation with:**

$$|\eta_e| < 2.47, E_{Te} > 15\,\mathrm{GeV}, |\eta_\mu| < 2.7, E_{T\mu} > 10\,\mathrm{GeV}$$

□**Jets: Anti-k$_t$ with R=0.4, overlap removal:**

$$|\eta_j| < 4.4, p_{Tj} > 30\,\mathrm{GeV}$$

□**B-jets with working points**

$$\epsilon_b(R_j) : 60\%(450), 70\%(140), 80\%(29), 85\%(11)$$

Diphoton Invariant Mass

- Primary vertex reconstruction :

  - Photon calorimeter pointing

  - Use conversion tracks when available

- Energy scale calibration from Z to electrons applied

- Crystal Ball + Gaussian model with narrow widths (of the core of the distribution) :

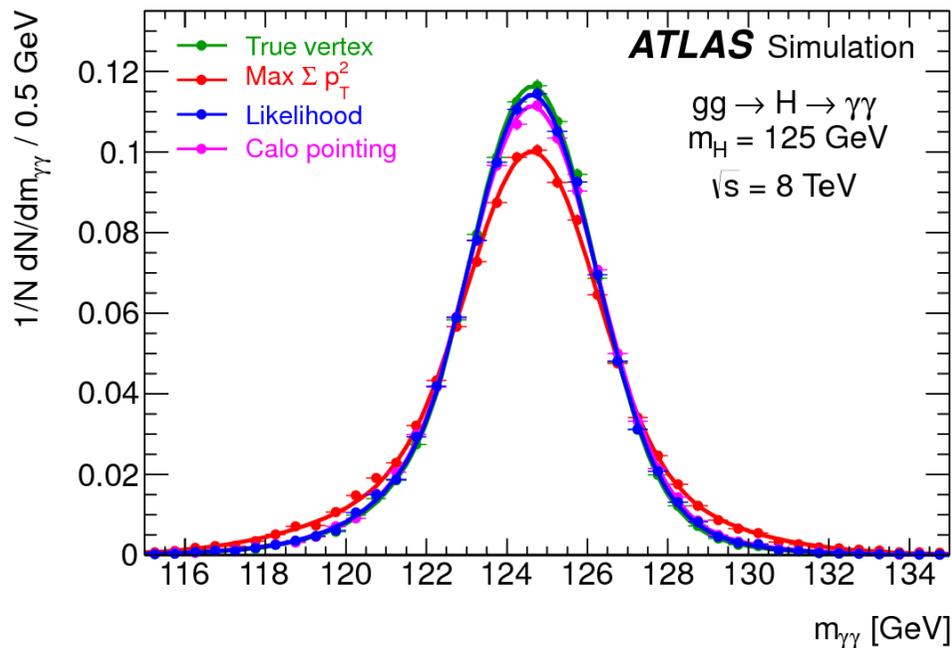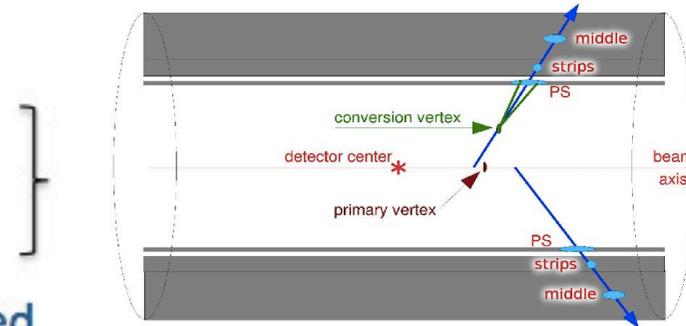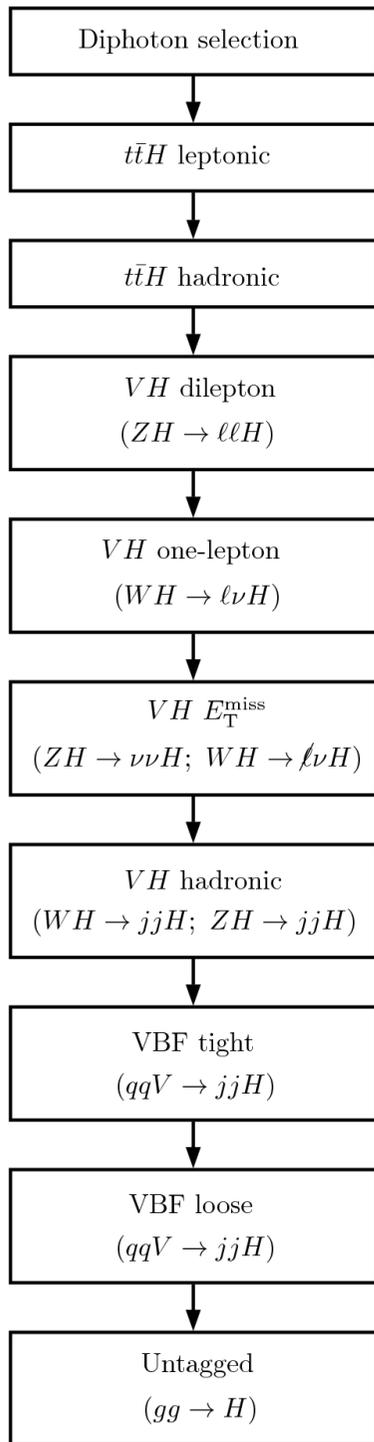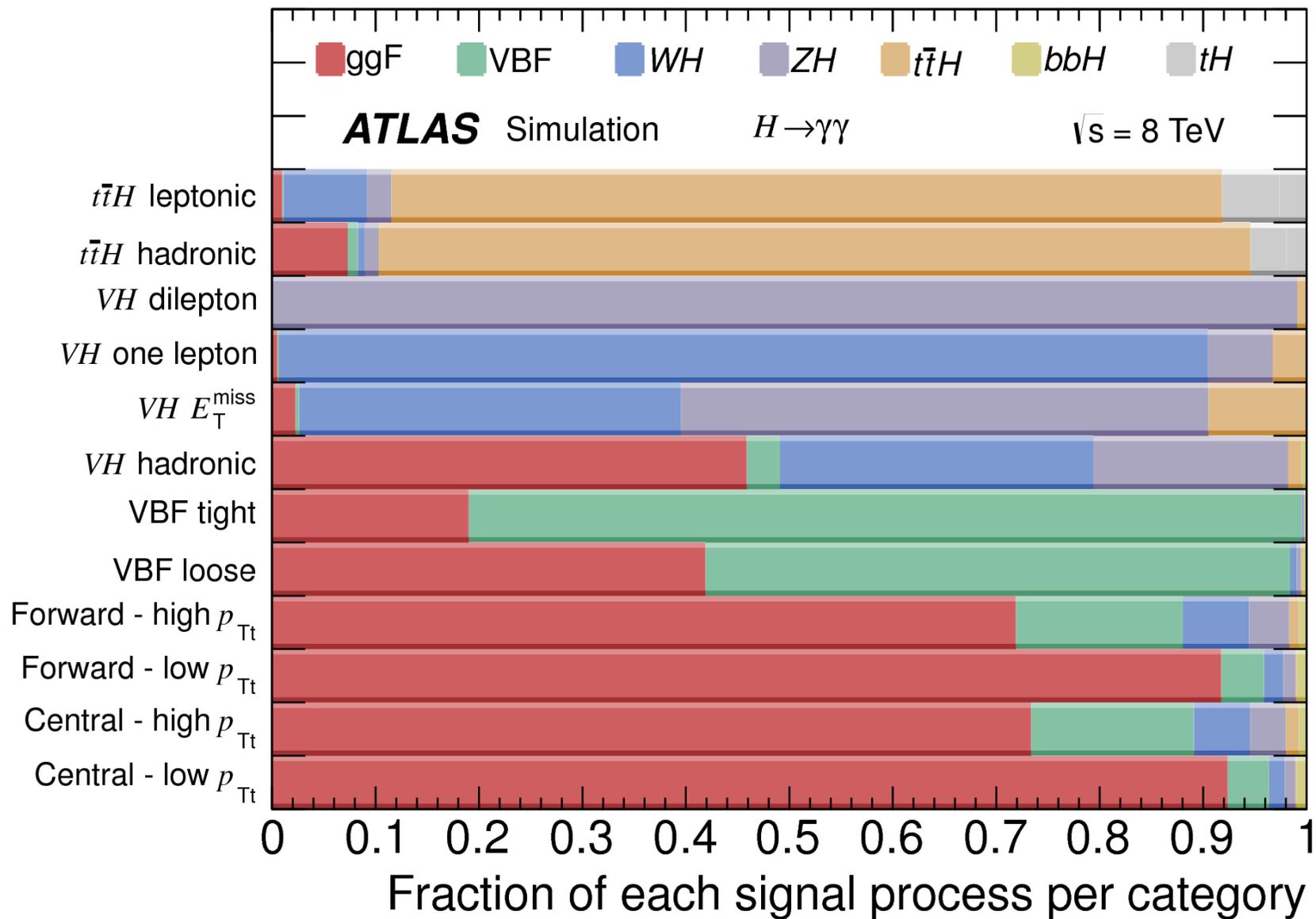**Introducing categories to enhance sensitivity to explore various production mechanisms**

Flowchart boxes (left):
- Diphoton selection
- $t\bar{t}H$ leptonic
- $t\bar{t}H$ hadronic
- VH dilepton $(ZH \to \ell\ell H)$
- VH one-lepton $(WH \to \ell\nu H)$
- VH E_T^{miss} $(ZH \to \nu\nu H; WH \to \ell\nu H)$
- VH hadronic $(WH \to jjH; ZH \to jjH)$
- VBF tight $(qqV \to jjH)$
- VBF loose $(qqV \to jjH)$
- Untagged $(gg \to H)$

Chart legend: ggF, VBF, WH, ZH, $t\bar{t}H$, bbH, tH

ATLAS Simulation $H \to \gamma\gamma$ $\sqrt{s} = 8$ TeV

Chart categories (y-axis):
$t\bar{t}H$ leptonic, $t\bar{t}H$ hadronic, VH dilepton, VH one lepton, VH E_T^{miss}, VH hadronic, VBF tight, VBF loose, Forward - high p_{Tt}, Forward - low p_{Tt}, Central - high p_{Tt}, Central - low p_{Tt}

X-axis: Fraction of each signal process per category

Phys. Rev. D 90, 112015 (2014)

8

Effective signal mass resolutions σ₆₈ and σ₉₀ for the 7 TeV and 8 TeV data in each event category, where σ₆₈ (σ₉₀) is defined as half of the smallest interval expected to contain 68% (90%) of the signal events
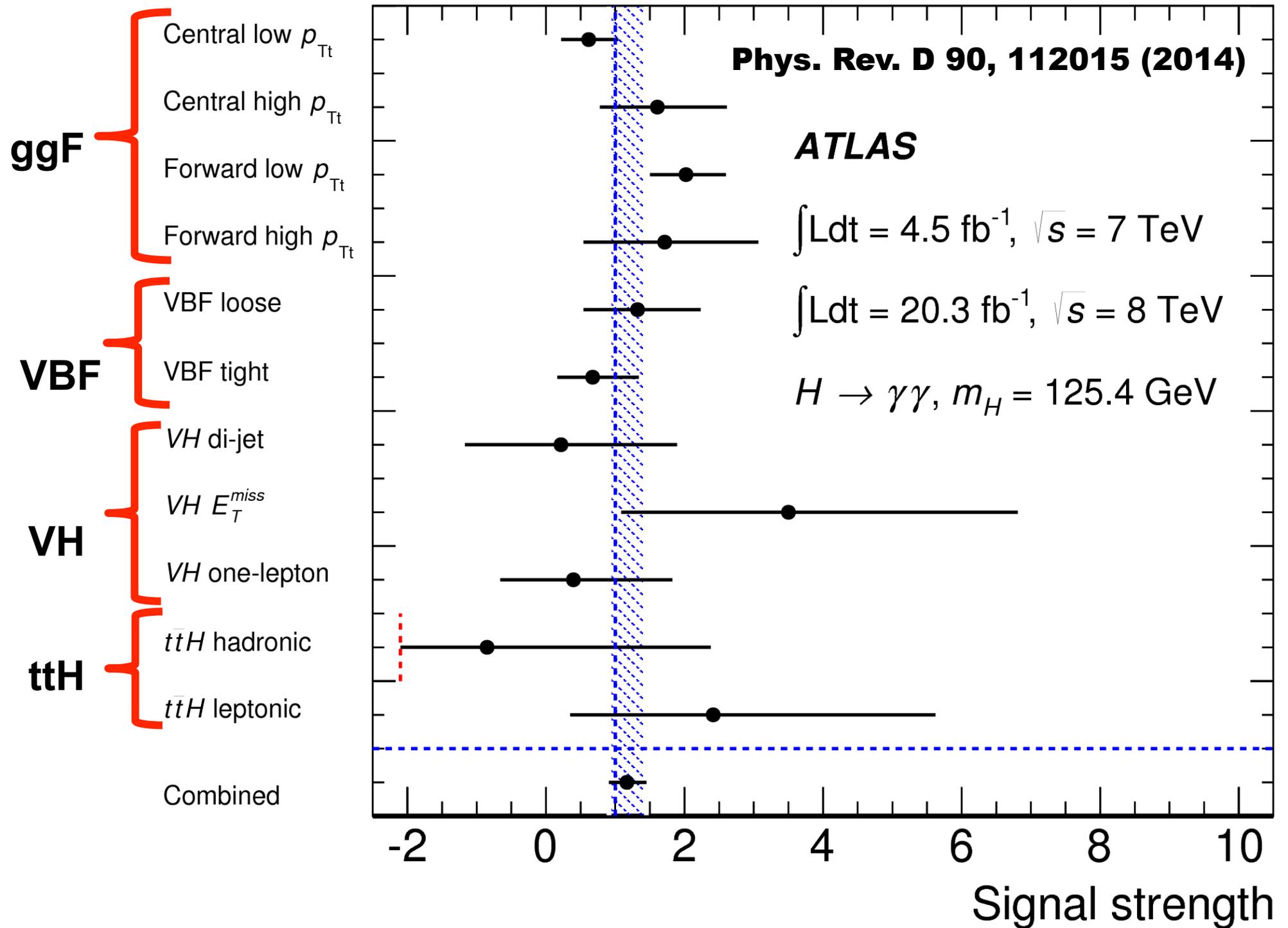
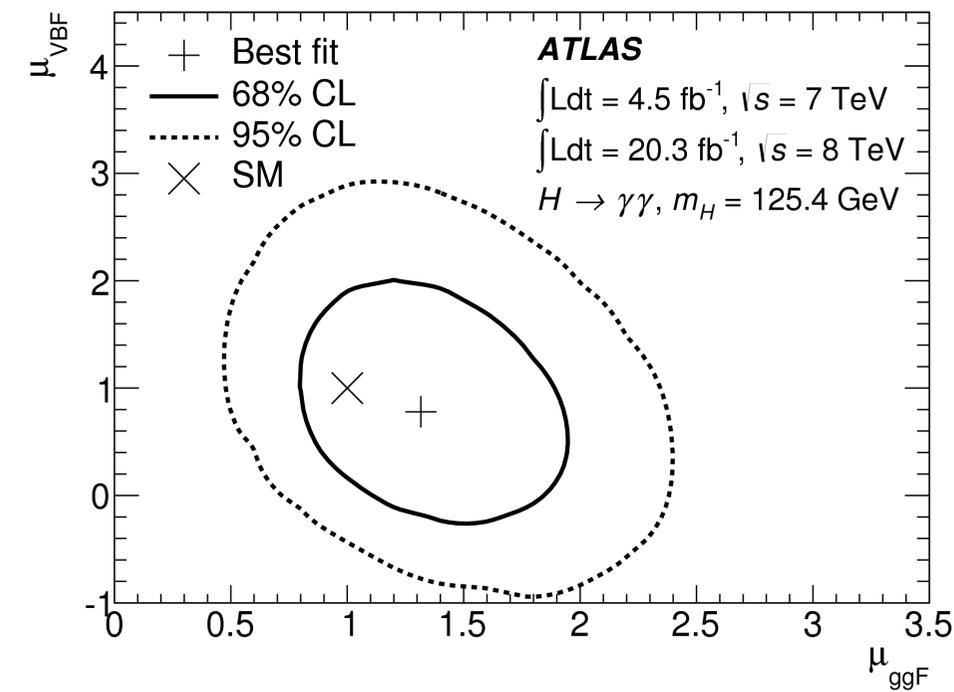| Category	$\sqrt{s}=7$ TeV		$\sqrt{s}=8$ TeV	
	σ_{68} [GeV]	σ_{90} [GeV]	σ_{68} [GeV]	σ_{90} [GeV]
Central - low p_{Tt}	1.36	2.32	1.47	2.50
Central - high p_{Tt}	1.21	2.04	1.32	2.21
Forward - low p_{Tt}	1.69	3.03	1.86	3.31
Forward - high p_{Tt}	1.48	2.59	1.64	2.88
VBF loose	1.43	2.53	1.57	2.78
VBF tight	1.37	2.39	1.47	2.61
VH hadronic	1.35	2.32	1.45	2.57
VH $E_{\mathrm{T}}^{\mathrm{miss}}$	1.41	2.44	1.56	2.74
VH one-lepton	1.48	2.55	1.61	2.80
VH dilepton	1.45	2.59	1.59	2.76
$t\bar{t}H$ hadronic	1.39	2.37	1.53	2.64
$t\bar{t}H$ leptonic	1.42	2.45	1.56	2.69

Signal Strengths
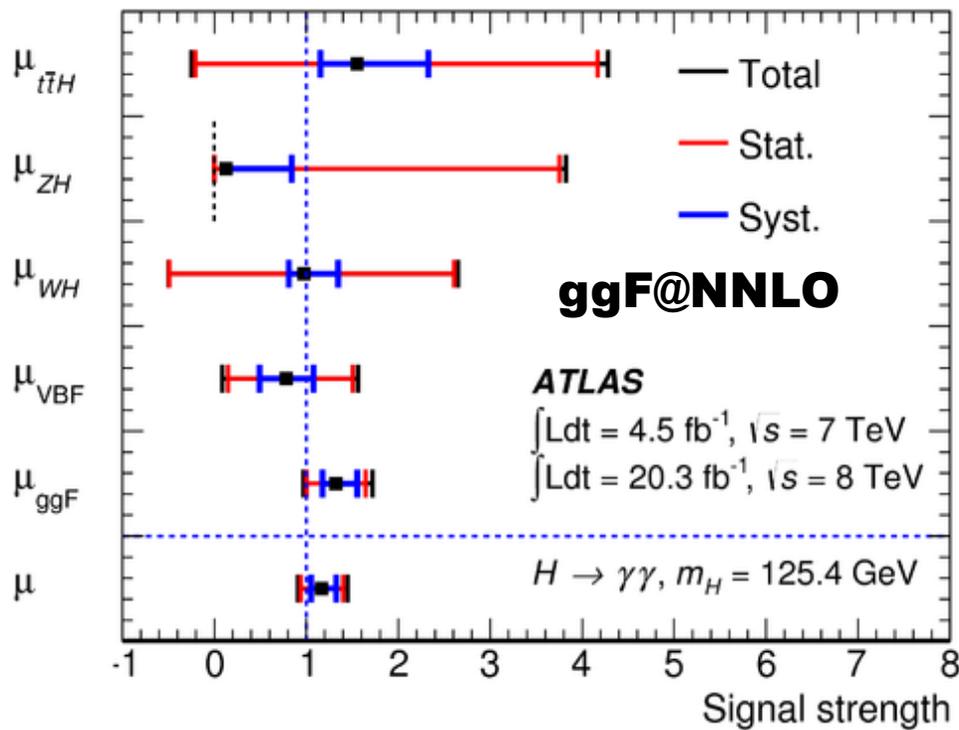
$$\mu_i = \frac{\sigma_i}{(\sigma_i)_{\text{SM}}} \quad \text{and} \quad \mu^f = \frac{B^f}{(B^f)_{\text{SM}}}$$

$$\mu_i^f = \frac{\sigma_i \cdot B^f}{(\sigma_i)_{\text{SM}} \cdot (B^f)_{\text{SM}}} = \mu_i \cdot \mu^f$$

Coupling Modifiers

$$\sigma_i \cdot B^f = \frac{\sigma_i(\vec{\kappa}) \cdot \Gamma^f(\vec{\kappa})}{\Gamma_H} \qquad \kappa_j^2 = \Gamma^j / \Gamma_{\text{SM}}^j$$
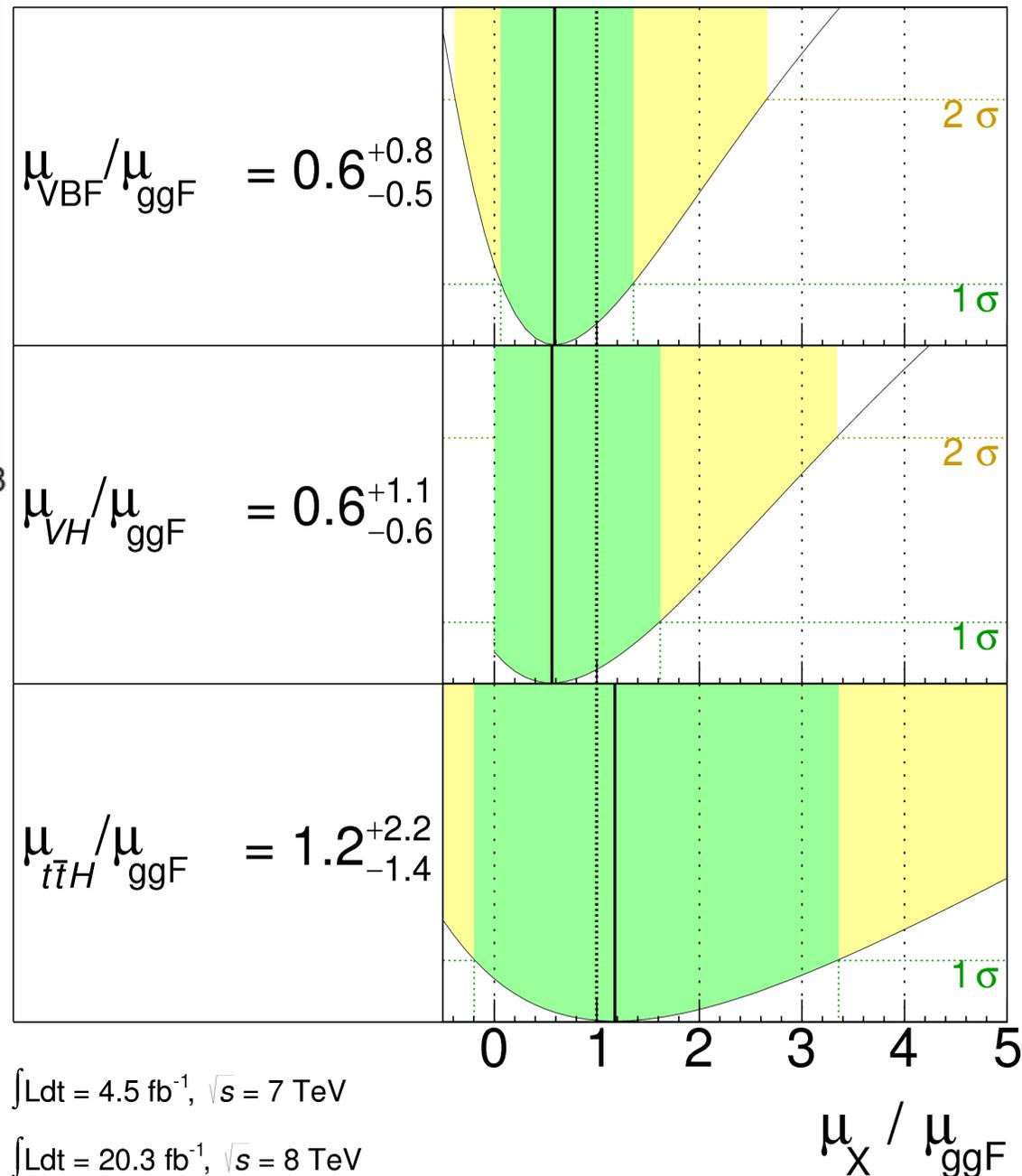
Systematics

Relative systematic uncertainties on the inclusive yields. Parentheses are for ttH and VH mechanisms

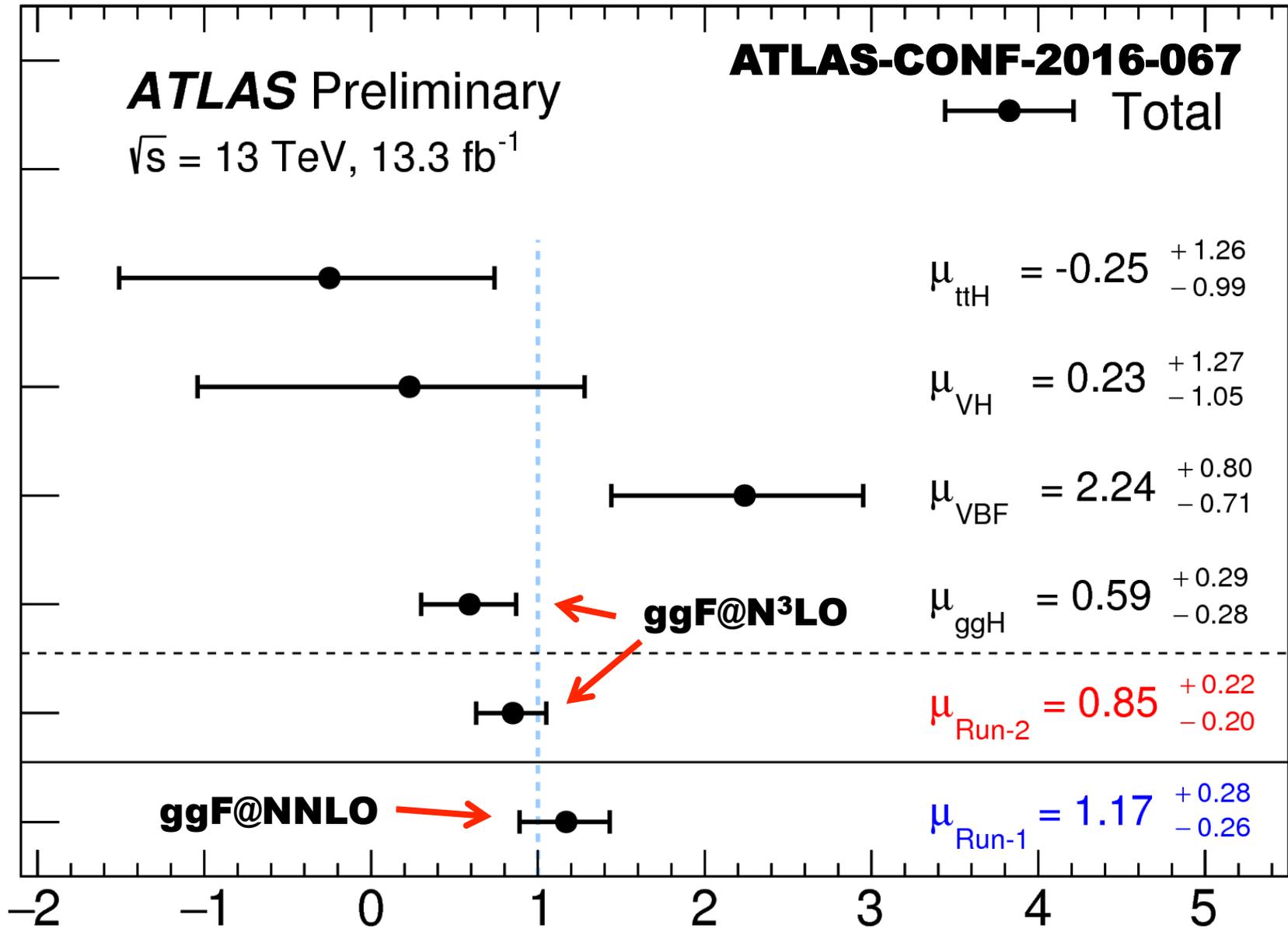| Uncertainty source	$\sqrt{s} = 7$ TeV	$\sqrt{s} = 8$ TeV
Luminosity	1.8	2.8
Trigger	0.2	0.2
Photon identification	8.4(9.3)	1.0(4.1)
Isolation	1.3–2.3(3.8)	1.3–2.3(3.8)

Systematic uncertainties on the diphoton mass resolution for the 8-TeV data. Used leading production mechanism in each category

Category	Constant term	Sampling term	Material modeling	Noise term
Central-low p_{Tt}	7.5	2.6	4.9	2.6
Central-high p_{Tt}	9.6	5.6	6.2	1.7
Forward-low p_{Tt}	9.9	1.3	6.0	2.1
Forward-high p_{Tt}	12	2.8	7.8	1.9
VBF loose	9.4	2.6	6.0	2.1
VBF tight	10	3.8	6.5	2.1
VH hadronic	11	4.0	7.2	1.6
VH E_T^{miss}	11	3.6	7.4	1.7
VH one-lepton	9.8	2.8	6.3	2.1
VH dilepton	9.5	2.7	6.2	2.1
$t\bar{t}H$ hadronic	9.6	3.6	6.3	1.9
$t\bar{t}H$ leptonic	9.5	3.4	6.2	2.1

Relative systematic uncertainties due to jet energy scale, jet energy resolution and jet vertex fraction

Category	ggF	VBF	$t\bar{t}H$	$WH + ZH$
Central + Forward-low p_{Tt}	0.1	2.9	4.0	0.1
Central + Forward-high p_{Tt}	1.1	4.5	3.5	1.4
VBF loose	12	4.4	7.6	13
VBF tight	13	9.1	6.3	17
VH hadronic	2.8	4.1	9.5	2.5
VH E_T^{miss}	2.6	9.0	1.2	0.2
VH one-lepton	4.9	6.2	2.8	0.5
VH dilepton	0	0	5.1	1.0
$t\bar{t}H$ hadronic	11	21	7.3	22
$t\bar{t}H$ leptonic	37	7.7	0.5	7.4

Fiducial and differential cross-sections

Measure detector-corrected event yields without imposing theory assumptions

Cross section in a fiducial region, or bin of a differential distribution

Number of signal events observed in the data

$$\sigma_i = \frac{\nu_i^{\text{sig}}}{c_i \int L \, dt}$$

Correction for detector resolution and inefficiency

Integrated luminosity of the dataset

JHEP09(2014)112
ATLAS-CONF-2016-067

The correction factors is the ratio of events reconstructed at detector-and particle-levels

15

Transverse momentum

Jet multiplicity

JHEP09(2014)112
ATLAS-CONF-2016-067

Effective Lagrangian approach

CP-even →

New HWW,HZZ, HZγ interactions

$$\mathcal{L}_{\text{eff}} = \bar{c}_\gamma O_\gamma + \bar{c}_g O_g + \boxed{\bar{c}_{HW} O_{HW} + \bar{c}_{HB} O_{HB}}$$
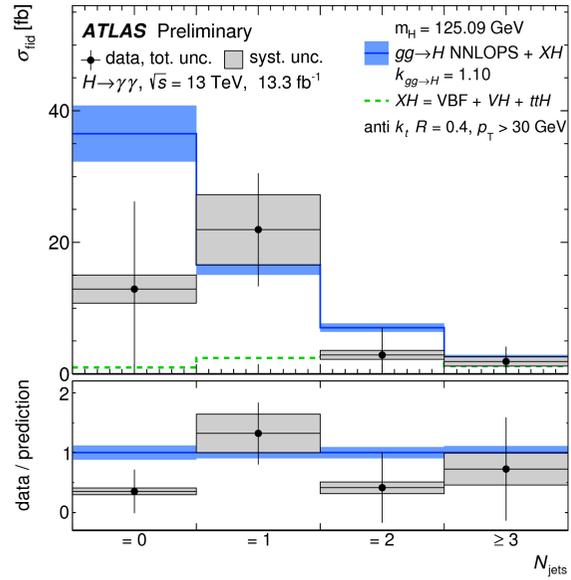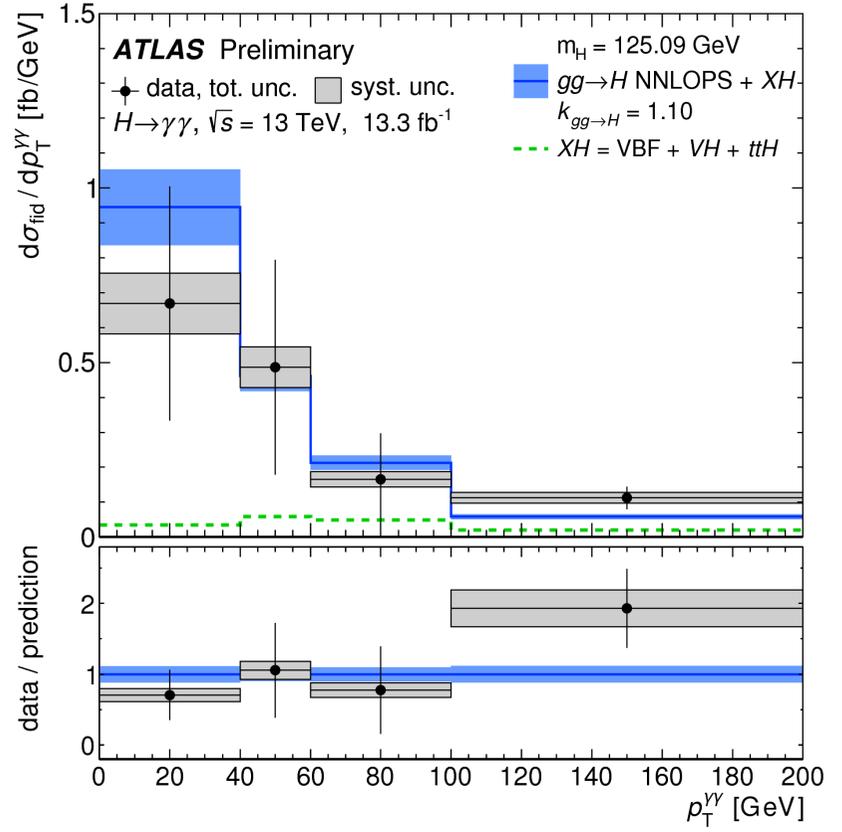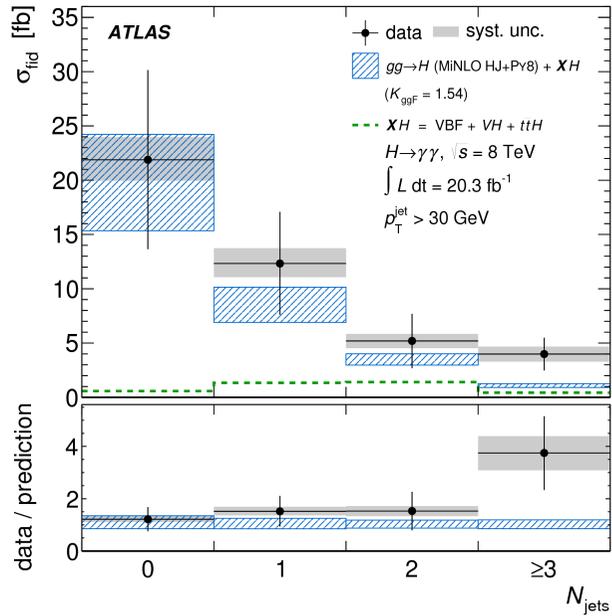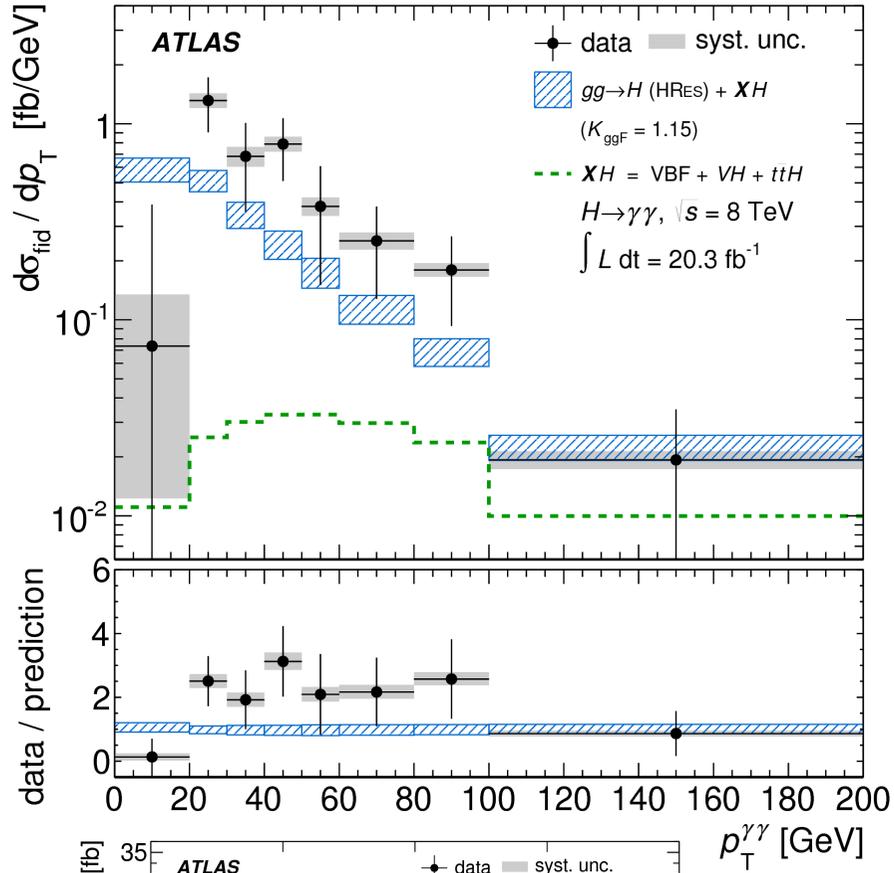$$+ \tilde{c}_\gamma \tilde{O}_\gamma + \tilde{c}_g \tilde{O}_g + \boxed{\tilde{c}_{HW} \tilde{O}_{HW} + \tilde{c}_{HB} \tilde{O}_{HB}}$$

CP-odd →

Sensitivity to signal strength and differential distributions

$$\frac{d\sigma}{dX} = \sum_j \left(\frac{d\sigma_j}{dX}\right)^{\text{ref}} \cdot \left(\frac{d\sigma_j}{dX}\right)^{\text{MG5}}_{c_i} \Bigg/ \left(\frac{d\sigma_j}{dX}\right)^{\text{MG5}}_{c_i=0}$$

LO Madgraph used to model effect of HD operators. Assume QCD/EW HO corrections factorize from NP

$pp \to H \to \gamma\gamma$, $\sqrt{s} = 8$ TeV, 20.3 fb^{-1}
ATLAS
- data
- Standard Model
- $\bar{c}_g = 0.0001$
- $\bar{c}_{HW} = 0.05$

Observed allowed ranges at 95% CL

Coefficient	$95\%\ 1 - CL$ limit
$\bar{c}_\gamma$	$[-7.4, 5.7]\times 10^{-4} \cup [3.8, 5.1]\times 10^{-3}$
$\tilde{c}_\gamma$	$[-1.8, 1.8]\times 10^{-3}$
$\bar{c}_g$	$[-0.7, 1.3]\times 10^{-4} \cup [-5.8, -3.8]\times 10^{-4}$
$\tilde{c}_g$	$[-2.4, 2.4]\times 10^{-4}$
$\bar{c}_{HW}$	$[-8.6, 9.2]\times 10^{-2}$
$\tilde{c}_{HW}$	$[-0.23, 0.23]$

Outlook and Conclusions

❑ **The di-photon final state plays a critical role in the understanding of the Higgs boson**

❑ **Signal strengths of different production mechanisms and their ratio to ggF are measured**

❑ **First fiducial total and differential cross-sections measured with Run I data**

❑ **Exploration of different production mechanisms a very important role for Run 2**

❑ **First measurements of signal strengths and fiducial cross-sections with Run 2 measured**

   ❑ **Looking forward to measurements with significantly larger Run 2 data sets**

Extra Slides

TABLE I. Summary of event generators and PDF sets used to model the signal and the main background processes. The SM cross sections σ for the Higgs production processes with $m_H = 125.4$ GeV are also given separately for $\sqrt{s} = 7$ TeV and $\sqrt{s} = 8$ TeV, together with the orders of the calculations.

Process	Generator	Showering	PDF set	Order of calculation	σ[pb] $\sqrt{s} = 7$ TeV	σ[pb] $\sqrt{s} = 8$ TeV
ggF	POWHEG-BOX	PYTHIA8	CT10	NNLO(QCD) + NLO(EW)	15.04	19.15
VBF	POWHEG-BOX	PYTHIA8	CT10	NLO(QCD + EW) + app.NNLO(QCD)	1.22	1.57
WH	PYTHIA8	PYTHIA8	CTEQ6L1	NNLO(QCD) + NLO(EW)	0.57	0.70
ZH	PYTHIA8	PYTHIA8	CTEQ6L1	NNLO(QCD) + NLO(EW)	0.33	0.41
$t\bar{t}H$	POWHEL	PYTHIA8	CT10	NLO(QCD)	0.09	0.13
$tHbj$	MADGRAPH	PYTHIA8	CT10	NLO(QCD)	0.01	0.02
tHW	MADGRAPH5_AMC@NLO	HERWIG++	CT10	NLO(QCD)	< 0.01	< 0.01
$b\bar{b}H$	$\cdots$	$\cdots$	$\cdots$	5FS(NNLO) + 4FS(NLO)	0.15	0.20
$\gamma\gamma$	SHERPA	SHERPA	CT10			
γ–jet	SHERPA	SHERPA	CT10			
jet jet	PYTHIA8	PYTHIA8	CTEQ6L1			

	σ_{68} [GeV]	σ_{90} [GeV]
Central low-$p_{\mathrm{T}t}$	1.60	2.72
Central high-$p_{\mathrm{T}t}$	1.39	2.36
Forward low-$p_{\mathrm{T}t}$	2.07	3.65
Forward high-$p_{\mathrm{T}t}$	1.84	3.22
VBF loose	1.68	2.96
VBF tight	1.53	2.73
VH hadronic loose	1.65	2.90
VH hadronic tight	1.49	2.61
VH $E_{\mathrm{T}}^{\mathrm{miss}}$	1.65	2.86
VH one-lepton	1.68	2.99
VH dilepton	1.73	2.99
$t\bar{t}H$ hadronic	1.60	2.87
$t\bar{t}H$ leptonic	1.65	2.85

Cross-section measurements

- First Higgs differential cross section results
- Follows closely the coupling analysis strategy
- Allows to probe kinematics of Higgs boson
- As model-independent as possible

**JHEP09(2014)112
ATLAS-CONF-2016-067**

Parton-level Inclusive

Fiducial Correction

Parton-level Fiducial

NP Correction

Particle-level Fiducial

Unfolding

Reco-level Fiducial

- Extract signal at reconstruction level
- Derive unfolding factors to unfold to particle level
- All results presented at particle level
- Also provide NP and fiducial correction factors for theorist use

23

Statistical correlations between the measured cross sections in bins of the diphoton transverse momentum and jet multiplicity distributions.

$pp \rightarrow H \rightarrow \gamma\gamma$, $\sqrt{s} = 8$ TeV, 20.3 fb^{-1}

ATLAS

Statistical correlation [%]

N_{jets}	0-20	20-30	30-40	40-50	50-60	60-80	80-100	100-200
≥ 3	2.8 ±1.0	2.0 ±1.0	5.2 ±1.0	5.2 ±1.0	7.9 ±1.0	10.4 ±1.0	10.5 ±1.0	20.9 ±1.0
$= 2$	4.7 ±1.1	7.3 ±1.1	9.0 ±1.0	9.7 ±1.0	12.7 ±1.0	22.5 ±0.9	21.6 ±1.0	20.5 ±1.0
$= 1$	7.7 ±1.0	14.3 ±1.1	23.0 ±1.1	29.4 ±0.9	28.6 ±0.9	30.0 ±0.9	19.4 ±1.0	15.3 ±1.0
$= 0$	74.8 ±0.5	40.1 ±1.0	23.0 ±1.2	12.5 ±1.2	4.1 ±1.0	3.7 ±1.0	-1.3 ±1.0	0.3 ±1.1

$p_T^{\gamma\gamma}$ [GeV]

PLB 753 (2016) 69-85

25

PLB 753 (2016) 69-85